Engineering and Technology Journal e-ISSN: 2456-3358

Volume 08 Issue 08 August -2023, Page No.- 2565-2571

DOI: 10.47191/etj/v8i8.10, I.F. – 7.136

Robust Super-Twisting Sliding Mode Control for Balancing Reaction Wheel Pendulum

Yusie Rizal[1], Syamsudin Noor[1], Sunu Hasta Wibowo[1], Sarifudin[1], Ronny Mantala[2], Ivan Maududy[1]

[1]Department of Electrical Engineering, Politeknik Negeri Banjarmasin, Banjarmasin, Indonesia

[2]Department of Business Administration, Politeknik Negeri Banjarmasin, Banjarmasin, Indonesia

ABSTRACT: Underactuated systems are one of the emerging research topics due to their challenging problems and applications in real-world engineering systems. In this paper, we consider the control problem of balancing the reaction wheel pendulum. Many control methods have been adopted to control the system and one of the common controls is based on sliding mode control (SMC). In SMC, the chattering phenomenon and its solution are widely discussed. Several approaches have been proposed, for example replacing the switching function, second-order SMC, and higher-order SMC. Here, the balancing of the reaction wheel pendulum with disturbances is considered. First, the system model derivation based on the Euler-Lagrange method is discussed. Second, a different approach to designing a controller is given where feedback linearization and robust super-twisting sliding mode control are used. The control performances are compared with those of standard and modified switching functions of first-order sliding mode control. For second-order sliding mode control, the super-twisting and PID super-twisting controllers are employed. In each controller, similar disturbances, namely, impulse signal and sinusoidal signal are used to verify the effectiveness of the controller. We conduct the comparison studies in Matlab/Simulink with fixed controller's gains and the controllers effectively stabilize the pendulum upright and reject the given external disturbances.

KEYWORDS: Reaction Wheel Pendulum; Sliding Mode Control; Balancing Control; Robust Super-Twisting Control

I. INTRODUCTION

A reaction wheel pendulum (RWP) is a two-degree of freedom (DOF) system where a rotating disk is actuated at one end of a pendulum while the other end of the pendulum is pivoted to the base. The system was first coined by Spong et al. [1], where he pointed out the simplicity of its dynamics among other similar pendulums yet nonlinear and underactuated. So far, the system has been used as a benchmark to study advanced methodologies in the nonlinear control system as well as to study the simplified model of decoupled systems. There are two common control problems in RWP, namely: (1) swing up and stabilize the pendulum in an inverted position, and (2) stabilize the pendulum upright from an initial position around an unstable equilibrium point. In this paper, we consider the control problem of stabilizing the pendulum in the upper position from an initial position near the equilibrium point. This control problem has practical applications in robotics, e.g. in 2 DOF robots with two links [2], reaction wheel unicycle robots [3],[4], and new spherical drive wheel robots [5].

In literature, many control methods have been proposed to solve this control problem using sliding mode control [6],[7],[8]. In [6], the second-order sliding mode control is used to track reference trajectory. In contrast, in [7], a combination of sliding mode control and generalized PI control is employed to solve the problem. A novel sliding mode control based on the quasi-chained form of coordinate transformation is presented in [8] in which the state variables vanish asymptotically towards the equilibrium point. Here, we present the comparison of balancing control of RWP using first-order and second-order sliding mode controls. In second-order sliding mode control (SOSMC), the control algorithms are based on the Super-Twisting algorithm (STA) and Adaptive Super-Twisting algorithm (ASTA). This work is different from those in [6],[7],[8] as well as in previous works in [3],[4]. The difference with existing control methods in [3],[4],[6],[7],[8],[9] can be described briefly in the following. Firstly, the sliding surface is defined based on the feedback linearization as given in [1],[10]. Secondly, two control algorithms i.e. STA and ASTA, as opposed to classical sliding mode control are compared in terms of control performance and chattering effect in control input.

Generally, there are two approaches to solve this stabilization control problem by using state-feedback linearization [1],[3],[4],[7],[10],[11], [12] and output feedback linearization [13],[14]. In this paper, we present comparative studies on different control algorithms in first-order and second-order sliding mode controls based on state-feedback linearization. It is well known that the disadvantage of classical first-order sliding mode control is introducing control chattering, while second-order sliding mode control can attenuate this effect. However, in recent studies of chattering parameters for first-order sliding mode control and the Super-

Twisting algorithm as discussed by Perez-Ventura and Fridman [15]: for a system with slow actuators, the amplitude of oscillations and average power produced by the Super-Twisting algorithm be larger than those one caused by first-order sliding mode control. Unlike the existing research discussed in [6],[7],[8],and [15], we compare the control performances and chattering effects of the said control algorithms for different scenarios by considering the changing sliding manifold parameters with the fixed controller gains.

We conduct several simulations for three control algorithms to stabilize the system using classical first-order sliding mode control, Super-Twisting algorithm, and Adaptive Super-Twisting algorithm. We observe the effect of choosing constant parameters in the sliding surface on the convergences of the system trajectory. Moreover, we provide simplification in the design stage by ignoring one term of system dynamics and considering this term as a perturbation. The control performances are evaluated and compared by treating similar initial positions and sliding surface parameters for all controllers. By choosing the same initial condition and sliding surface parameters, we expect the comparison between these control methods to become fair and unbiased. This work aims to provide a comparative study of different algorithms in second-order sliding mode control (using STA and ASTA) and first-order sliding mode control concerning the stabilization control of the reaction wheel pendulum.

II. REACTION WHEEL PENDULUM SYSTEM

A. System Model

Fig. 1 shows the system model of a reaction wheel pendulum. It consists of a reaction wheel or a disk and a pendulum where one side of the pendulum is attached to the base and the other side is connected to the reaction wheel. The system model can be derived as follows [11].

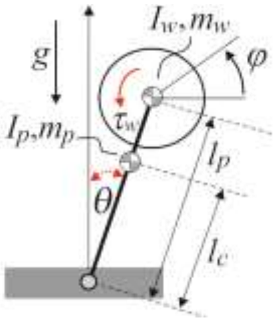

Fig. 1.System model of reaction wheel pendulum.

Let the pendulum position of the center of mass x_p and position of reaction wheel x_w are

$$x_p = l_c\,\theta \qquad x_w = l_p\,\theta \tag{1}$$

The kinetic energy of the pendulum and reaction wheel are

$$T_{tran} = \frac{1}{2} m_p \dot{x}_p^2 + \frac{1}{2} m_p \dot{x}_w^2 \tag{2}$$

$$T_{rot} = \frac{1}{2} I_p \dot{\theta}^2 + \frac{1}{2} I_w \left(\dot{\theta} + \dot{\varphi}\right)^2 \tag{3}$$

and the total kinetic energy T is

$$T = \frac{1}{2}\left(I_p + I_w + m_p l_c^2 + m_w l_p^2\right)\dot{\theta}^2 + \frac{1}{2} I_w \dot{\varphi}^2 + I_w \dot{\theta}\dot{\varphi} \tag{4}$$

while the energy potential is

$$V = \left(m_p l_c + m_w l_p\right) g \left(\cos\theta - 1\right) \tag{5}$$

The Lagrangian function is given by

$$L = T - V \tag{6}$$

Thus, the Euler-Lagrange is

$$\frac{\partial}{\partial t}\left(\frac{\partial L}{\partial \dot{q}}\right) - \frac{\partial L}{\partial q} = Q \tag{7}$$

Where

$$q^T = \begin{bmatrix}\theta & \varphi\end{bmatrix} \tag{8}$$

$$Q^T = \begin{bmatrix}0 & \tau_w\end{bmatrix} \tag{9}$$

By rearranging the equations, we have:

$$\begin{aligned} &\left(I_p + I_w + m_p l_c^2 + m_w l_p^2\right)\ddot{\theta} + I_w \ddot{\varphi} - \tilde{m}\, g \sin\theta = 0 \\ &I_w \ddot{\theta} + I_w \ddot{\varphi} = \tau_w \end{aligned} \tag{10}$$

Where

$$\tilde{m} = l_c m_p + l_p m_w \tag{11}$$

With the system parameters are given in Table I.

Table I. Parameter of the System

Symbol	Description	Value	S.I. Unit
m_p	Pendulum’s mass	0.141	kg
m_w	Reaction wheel’s mass	0.554	kg
I_p	Pendulum’s moment inertia	0.69×10^{-3}	$kg.m^2$
I_w	Reaction wheel’s moment inertia	4.36×10^{-3}	$kg.m^2$
l_c	Center of mass of pendulum	0.11	m
l_p	Length of pendulum	0.21	m
g	Gravity acceleration	9.81	$kg.m/s^2$
τ_w	Torque (control) input	-	N.m

We use the state-variables of the system:

$$x_1 = \theta,\ x_2 = \dot{\theta},\ x_3 = \varphi,\ x_4 = \dot{\varphi} \tag{13}$$

and thus, we have

$$\dot{x} = f(x) + g(x)u \tag{14}$$

where the states $x \in D \subset \Re^n$, input $u \in U \subset \Re^m$ and $f(x)$ and $g(x)$ are locally Lipschitz.

$$f(x) = \begin{pmatrix} x_2 \\ a_{22}\tilde{m}\, g \sin x_1 / d \\ x_4 \\ -a_{21}\tilde{m}\, g \sin x_1 / d \end{pmatrix}, g(x) = \begin{pmatrix} 0 \\ -a_{12}/d \\ 0 \\ a_{11}/d \end{pmatrix} \tag{15}$$

with a_{11}, a_{12}, a_{21}, a_{22}, and d are:

$$\begin{aligned} a_{11} &= I_p + I_w + m_p l_c^2 + m_w l_p^2 \\ a_{12} &= a_{21} = a_{22} = I_w \\ d &= I_w\left(I_p + m_p l_c^2 + m_w l_p^2\right) \end{aligned} \tag{16}$$

From the analysis of the system in (10), we obtain the phase potrait of the pendulum as given in Fig. 2 where each set of initial conditions is represented by a different point or curve.

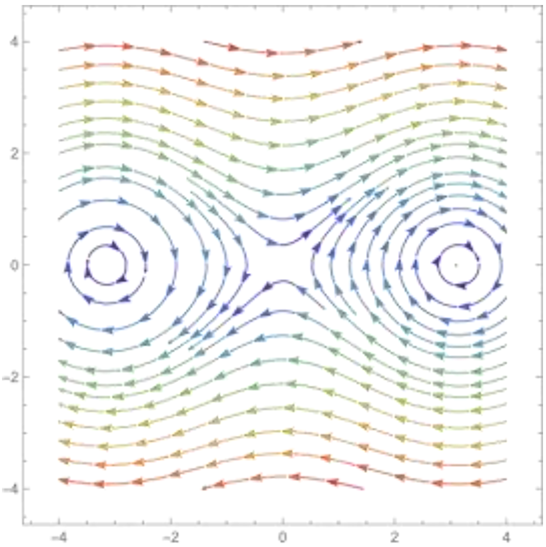

Fig. 2.Phase portrait of the pendulum

B. Controllability and Involutivity Conditions

To check the controllability and involutivity of the system, first, we simplify the system by ignoring the third state variable x_3 in Eq. (14) due to the cyclic-variable [10]. From Eq. (15), we have

$$f(x) = \begin{pmatrix} x_2 \\ a_{22}\tilde{m}\, g \sin x_1 / d \\ -a_{21}\tilde{m}\, g \sin x_1 / d \end{pmatrix}, g(x) = \begin{pmatrix} 0 \\ -a_{12}/d \\ a_{11}/d \end{pmatrix} \tag{17}$$

For short, we use f and g for $f(x)$ and $g(x)$, respectively. We calculate the rank of the system in Eq. (14),

$$Rank\begin{bmatrix} ad_f^0 g & ad_f^1 g & ad_f^2 g \end{bmatrix} = 3 \tag{18}$$

i.e. full rank, where the elements in Eq. (18) are given in the following as the results of Lie Brackets

$$ad_f^0 g = g = \begin{bmatrix} 0 \\ -a_{12}/d \\ a_{11}/d \end{bmatrix} \tag{19}$$

$$ad_f^1 g = [f, g] = \nabla g \cdot f - \nabla f \cdot g = \begin{bmatrix} a_{12}/d \\ 0 \\ 0 \end{bmatrix} \tag{20}$$

$$\begin{aligned} ad_f^2 g &= \left[f, ad_f^1 g\right] = \nabla(ad_f^1 g)\cdot f - \nabla f \cdot (ad_f^1 g) \\ &= \begin{bmatrix} 0 \\ -a_{12}a_{22}\tilde{m}g \cos x_1 / d^2 \\ a_{12}a_{21}\tilde{m}g \cos x_1 / d^2 \end{bmatrix} \end{aligned} \tag{21}$$

in which $[f, g]$ is a Lie Brackets. From Eq. (18) we obtained the system is controllable.

Next, we check the involutivity of the system in Eq. (15) using

$$\begin{bmatrix} g & ad_f g \end{bmatrix} \tag{22}$$

$$Rank\left[f_1 \;\; f_2\right] = Rank\left[f_1 \;\; f_2 \;\; [f_1, f_2]\right] \tag{23}$$

since,

$$[f_1, f_2] = \nabla(ad_f g)\cdot g - \nabla g \cdot (ad_f g) = \begin{bmatrix} 0 & 0 & 0 \end{bmatrix} \tag{24}$$

and hence,

$$\begin{aligned} &Rank\begin{bmatrix} 0 & a_{12}/d \\ -a_{12}/d & 0 \\ a_{11}/d & 0 \end{bmatrix} \\ &= Rank\begin{bmatrix} 0 & a_{12}/d & 0 \\ -a_{12}/d & 0 & 0 \\ a_{11}/d & 0 & 0 \end{bmatrix} \end{aligned} \tag{25}$$

i.e., the rank is 3.

We want to find the output function that can lead us to the input-output linearization with relative degree n. We assume that y is the output that we are looking for. By using the following procedure, we then try to find the solution for y.

$$\begin{aligned} \nabla y \cdot (ad_f^0 g) &= 0 \\ \nabla y \cdot (ad_f^1 g) &= 0 \\ \nabla y \cdot (ad_f^2 g) &\neq 0 \end{aligned} \tag{26}$$

in which, $\nabla y \cdot (ad_f^0 g) = -\dfrac{a_{12}}{d}\dfrac{\partial y}{\partial x_2} + \dfrac{a_{11}}{d}\dfrac{\partial y}{\partial x_4} = 0$ (27)

$$\nabla y \cdot (ad_f^1 g) = \frac{a_{12}}{d}\frac{\partial y}{\partial x_1} = 0 \tag{28}$$

$$\nabla y \cdot (ad_f^2 g) = \nabla y \cdot \begin{bmatrix} 0 \\ -a_{12}a_{22}\tilde{m}g \cos x_1 / d^2 \\ a_{12}a_{21}\tilde{m}g \cos x_1 / d^2 \end{bmatrix} \neq 0 \tag{29}$$

The solution of (27)–(29) is

$$y = a_{11}x_2 + a_{12}x_4. \tag{30}$$

III. FEEDBACK LINEARIZATION

The control method used in this paper is based on feedback linearization. We compare different sliding mode control including standard feedback linearization. Let's suppose from Eq. (30),

$$h(x) = y \tag{31}$$

By taking Lie derivative for h with respect to f and g until we find $L_g L_f^{i-1} h \neq 0$, where for i=3 we have

$$L_g L_f^2 h = -\frac{\tilde{m} g a_{22} \cos x_1}{d} \neq 0 \tag{32}$$

This means for $i = 1,2$, we have

$$L_g L_f^0 h = L_g L_f^1 h = 0 \tag{33}$$

By denoting

$$\begin{aligned} \xi_1 &= a_{11} x_2 + a_{12} x_4 \\ \xi_2 &= \tilde{m} g \sin x_1 \\ \xi_3 &= \tilde{m} g x_2 \cos x_1 \end{aligned} \tag{34}$$

then, the first derivative of (34) are given as follow

$$\begin{aligned} \dot{\xi}_1 &= \xi_2 \\ \dot{\xi}_2 &= \xi_3 \\ \dot{\xi}_3 &= L_f^3 h + L_g L_f^2 h u \end{aligned} \tag{35}$$

where

$$L_f^3 h = -\tilde{m}\, g\, x_2^2 \sin x_1 + \frac{(\tilde{m}\, g)^2 a_{22} \cos x_1 \sin x_1}{d} \tag{36}$$

and by using u as

$$u = \tilde{m}\, g \sin x_1 - \frac{d\left(\nu + \tilde{m}\, g\, x_2^2 \sin x_1\right)}{\tilde{m}\, g\, a_{22} \cos x_1} \tag{37}$$

Hence, it follows from Eq. (35)

$$\begin{aligned} \dot{\xi}_1 &= \xi_2 \\ \dot{\xi}_2 &= \xi_3 \\ \dot{\xi}_3 &= \nu \end{aligned} \tag{38}$$

in which Eq. (38) is the feedback linearized form.

IV. CONTROLLER DESIGN

The controller design is presented in this section. Let's suppose the PID sliding surface [16] is

$$s = w_1 \xi_1 + w_2 \xi_2 + w_3 \xi_3 + k_i \int \left(\xi_1 + \xi_3\right) dt \tag{39}$$

By taking first derivative of Eq. (39), we have

$$\dot{s} = w_1 \dot{\xi}_1 + w_2 \dot{\xi}_2 + w_3 \dot{\xi}_3 + k_i \left(\xi_1 + \xi_3\right) \tag{40}$$

It follows that

$$\dot{s} = k_i \xi_1 + w_1 \xi_2 + \xi_3 \left(k_i + w_2\right) + w_3 \nu \tag{41}$$

The PID Super-Twisting sliding mode control is given by

$$\tau_1 = -\frac{1}{w_3}\left(\tau_{1eq} + \tau_{1st}\right) \tag{42}$$

where

$$\tau_{1eq} = k_i \xi_1 + w_1 \xi_2 + \left(k_i + w_2\right) \xi_3 \tag{43}$$

$$\tau_{1st} = \sigma_1 \sqrt{s}\, sign(s) + \sigma_2\, sign(s) \tag{44}$$

In comparison, we use a standard Super-Twisting algorithm [9], i.e. given by

$$\nu = \frac{1}{c_3}\left(\tau_{eq} + \tau_{st}\right) \tag{45}$$

Where

$$\tau_{eq} = -c_1 \xi_2 - c_2 \xi_3 \tag{46}$$

$$\tau_{st} = -k_1 |s|^{1/2} sign(s) - k_2 \int sign(s) \tag{47}$$

Moreover, for standard SMC, we use the control law as given in (45), where

$$\tau_{st} = -\eta\, sign(s). \tag{48}$$

For the modified switching function for SMC, the control law is [17]

$$\tau_{st} = -\gamma \tanh(s) \tag{49}$$

Where the equivalent control for Eq. (48) and (49) are similar as given

$$\tau_{eq} = -k_1 \xi_2 - k_2 \xi_3 \tag{50}$$

V. SIMULATION RESULTS

This section presents the simulation results that are obtained from Matlab/Simulink. In the simulation, we compare different control methods, namely, feedback linearization, standard sliding mode control, modified switching function of sliding mode control [17], Super-Twisting algorithm [18], and PID Super-Twisting controller. The control gains for each controller are given as follows. For feedback linearization, the control gains are $k_1 = 0.25$, $k_2 = 6$, and $k_3 = 3.5$. For the standard sliding mode control, we use control gains $k_1 = 1.5$, $k_2 = 20$, and $\eta = 30$, while the modified switching function SMC are $k_1 = 1.5$, $k_2 = 50.5$, and $\gamma = 30$. Furthermore, for the Super-Twisting algorithm, we choose c_1, c_2, c_3, k_1, and k_2 are 0.05, 15, 25, 20, and 25, respectively. Finally, for the PID Super-Twisting control gains w_1, w_2, w_3, k_i, σ_1, and σ_2 are given by 0.5, 60, 90, 0.01, 15, and 20, respectively.

The simulation results are presented in Figs. (3)–(7). In Fig. 3, the comparison of different controllers is given for the system without any disturbances. Based on the given controller gains, the modified SMC and standard SMC are the controllers that have fast convergences compared to the other controllers. Standard Super-Twisting and PID Super-Twisting have similar responses, while feedback linearization is moderate.

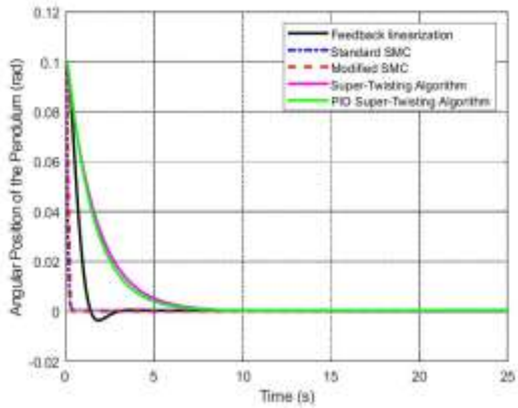

Fig. 3.Simulation of reaction wheel pendulum without disturbances

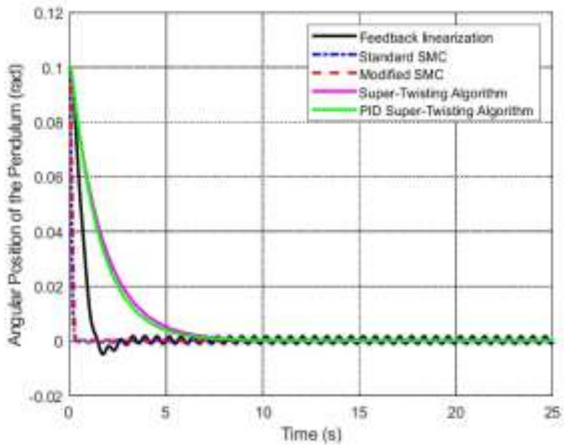

Fig. 4.Simulation of reaction wheel pendulum with sinusoidal disturbances.

In Fig. 4, the sinusoidal signal is given as a continuous disturbance. The amplitude for the disturbance is similar for all controllers, i.e., 0.0045 N/m with a frequency of 10 rad/sec. From the simulation result, as shown in Figs. 4 and 5, modified SMC, Standard, and PID Super-Twisting controllers have shown their robustness to reject sinusoidal disturbance.

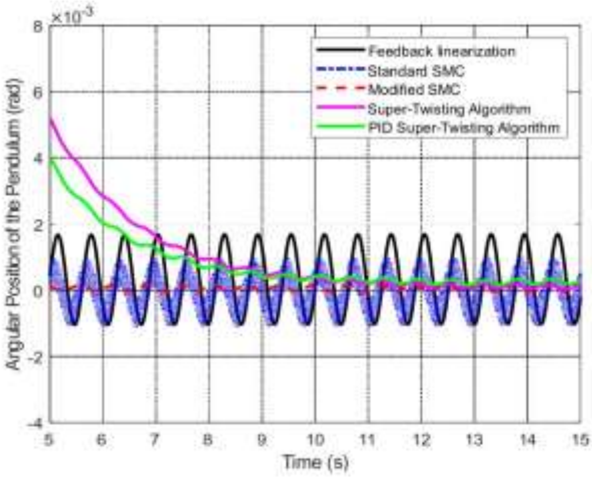

Fig. 5.Comparison of system responses for different control methods with sinusoidal disturbances.

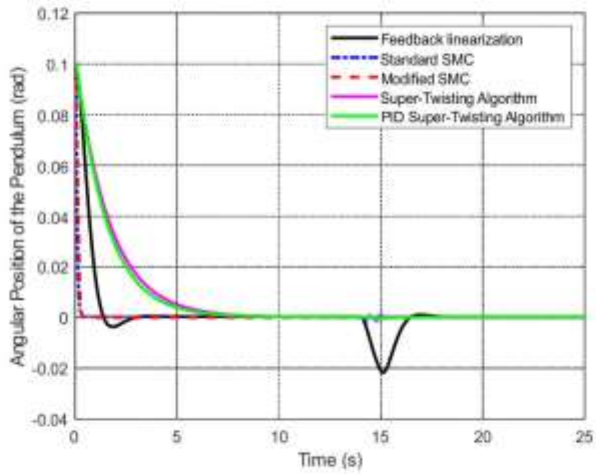

Fig. 6.Simulation results of reaction pendulum system with impulse disturbances.

To evaluate its robustness, another type of disturbance, i.e. impulse signal is introduced in the system. The amplitude of this disturbance signal is 0.005 N/m. The results are shown in Fig. 6 and 7. From these figures, the modified SMC and Standard Super-Twisting controller have shown their robustness to reject impulse disturbance. Among the others, feedback linearization control has the worst performance compared to the other four controllers when the system has disturbances.

Finally, the control performances are given in Tabel II-IV. Four criteria are used to measure its performance, i.e. Integral Absolute Error (IAE), Integral Time Absolut Error (ITAE), Integral Square Error (ISE), and Integral Time Square Error (ITSE).

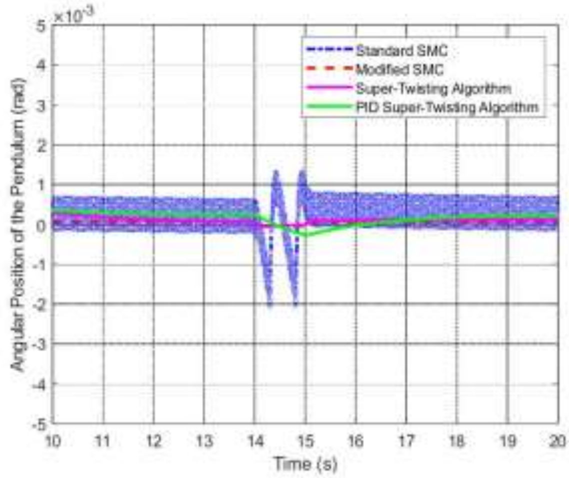

Fig. 7.Comparison of system response for different control methods with impulse disturbances.

Fig. 8.

Table II. Control Performances for System without disturbance

Control Method	Name of Criterion			
	IAE	ITAE	ISE	ITSE
Feedback Linearization	0.0828	0.5080	0.004 4	0.001 4
Standard	0.0405	0.7686	0.000	0.000

Control Method	Name of Criterion			
	IAE	ITAE	ISE	ITSE
SMC			7	7
Modified SMC	0.1607	0.0748	0.0009	0.0000
Standard STA	0.1725	0.3291	0.0088	0.0073
PID-STA	0.1703	0.6156	0.0082	0.0064

Table III. Control Performances for System with Sinusoidal Disturbance

Control Method	Name of Criterion			
	IAE	ITAE	ISE	ITSE
Feedback Linearization	0.1054	1.1470	0.0042	0.0025
Standard SMC	0.0437	0.8649	0.0007	0.0009
Modified SMC	0.0165	0.0844	0.0009	0.0000
Standard STA	0.1737	0.3738	0.0087	0.0073
PID-STA	0.1691	0.6097	0.0081	0.0063

From the simulation results as given in Tables II, II, and IV, we found that the values of IAE and ITAE are smaller when the controlled system has fast convergence. However, ISE and ITSE values will be smaller if the controlled system has a smaller steady-state error and fast convergence at the same time. It is shown in those tables with given controller gains, that the modified SMC has a better performance compared to the other controllers.

Table IV. Control Performances for System with Impulse Disturbance

Control Method	Name of Criterion			
	IAE	ITAE	ISE	ITSE
Feedback Linearization	0.1029	0.7195	0.0047	0.0073
Standard SMC	0.0413	0.7763	0.0007	0.0007
Modified SMC	0.0160	0.0741	0.0009	0.0000
Standard STA	0.1752	0.4184	0.0088	0.0073
PID-STA	0.1696	0.6038	0.0082	0.0064

VI. CONCLUSION

This paper studies the comparison of various nonlinear robust controllers using five different control algorithms, namely, the feedback linearization control, standard sliding mode control, modified switching function of first-order sliding mode control, a Super-Twisting controller, and PID Super-Twisting controller. All controllers have shown their effectiveness in stabilizing the reaction wheel pendulum system to balance upright. For the given controller gains, we found that the modified SMC has a better performance compared to the other four controllers.

ACKNOWLEDGMENT

The authors would like to thank P3M Politeknik Negeri Banjarmasin for funding this research and publication.

REFERENCES

1. M. W. Spong, P. Corke, and R. Lozano, "Nonlinear control of the Reaction Wheel Pendulum," *Automatica*, vol. 37, no. 11, pp. 1845–1851, 2001, doi: 10.1016/S0005-1098(01)00145-5.
2. S. Krafes, Z. Chalh, and A. Saka, "A Review on the Control of Second Order Underactuated Mechanical Systems," *Complexity*, vol. 2018, pp. 1–17, 2018.
3. Y. Rizal, C.-T. Ke, and M.-T. Ho, "Point-to-point motion control of a unicycle robot: Design, implementation, and validation," in *2015 IEEE International Conference on Robotics and Automation (ICRA)*, May 2015, pp. 4379–4384. doi: 10.1109/ICRA.2015.7139804.
4. G. P. Neves, B. A. Angélico, and C. M. Agulhari, "Robust H2 controller with parametric uncertainties applied to a reaction wheel unicycle," *Int. J. Control*, pp. 1–11, 2019, doi: 10.1080/00207179.2018.1562224.
5. N. Raja Sekhar, M. Korrapati, R. Hota, and C. Siva Kumar, "New Dynamic Model and Simulation of the Ballbot Using Reaction Wheels," in *Machines, Mechanism and Robotics*, D. N. Badodkar and T. A. Dwarakanath, Eds. Singapore: Springer Singapore, 2019, pp. 807–816. doi: 10.1007/978-981-10-8597-0_69.
6. R. Iriarte, L. T. Aguilar, and L. Fridman, "Second order sliding mode tracking controller for inertia wheel pendulum," *J. Franklin Inst.*, vol. 350, no. 1, pp. 92–106, 2013, doi: 10.1016/j.jfranklin.2012.10.013.
7. V. M. Hernandez, "A Combined Sliding Mode-Generalized Pi Control Scheme for Swinging Up and Balancing the Inertia Wheel Pendulum," *Asian J. Control*, vol. 5, no. 4, pp. 620–625, 2003.
8. N. Sun, Y. Fang, and H. Chen, "A Novel sliding mode control method for an inertia wheel pendulum system," in *2015 International Workshop on Recent Advances in Sliding Modes (RASM)*, Apr. 2015, pp. 1–6. doi: 10.1109/RASM.2015.7154585.
9. Y. Rizal, R. Mantala, S. Rachman, and N. Nurmahaludin, "Balance Control of Reaction Wheel Pendulum Based on Second-order Sliding Mode

Control," in *2018 International Conference on Applied Science and Technology (iCAST)*, Oct. 2018, pp. 51–56. doi: 10.1109/iCAST1.2018.8751548.

10. I. Fantoni and L. Rogelio, "The reaction wheel pendulum," in *Non-linear Control for Underactuated Mechanical Systems*, London: Springer, 2002, pp. 89–106.
11. I. Fantoni, R. Lozano, and M. W. Spong, "Stabilization of the Reaction Wheel Pendulum Using An Energy Approach," in *European Control Conference*, 2001, pp. 2552–2557.
12. A. Zhang, C. Yang, S. Gong, and J. Qiu, "Nonlinear stabilizing control of underactuated inertia wheel pendulum based on coordinate transformation and time-reverse strategy," *Nonlinear Dyn.*, vol. 84, no. 4, pp. 2467–2476, 2016, doi: 10.1007/s11071-016-2658-8.
13. N. Khalid and A. Y. Memon, "Output feedback stabilization of an Inertia Wheel Pendulum using Sliding Mode Control," in *International Conference on Control*, 2014, no. July, pp. 157–162. doi: 10.1109/CONTROL.2014.6915132.
14. N. Khalid and A. Y. Memon, "Output Feedback Control of a Class of Under-Actuated Nonlinear Systems Using Extended High Gain Observer," *Arab. J. Sci. Eng.*, vol. 41, no. 9, pp. 3531–3542, 2016, doi: 10.1007/s13369-016-2144-0.
15. U. Pérez-ventura and L. Fridman, "Chattering Comparison Between Continuous and Discontinuous Sliding-Mode Controllers," in *Variable-Structure Systems and Sliding-Mode Control*, Springer, 2020, pp. 197–211. doi: 10.1007/978-3-030-36621-6.
16. F. F. M. El-Sousy, K. A. Alattas, O. Mofid, S. Mobayen, and A. Fekih, "Robust Adaptive Super-Twisting Sliding Mode Stability Control of Underactuated Rotational Inverted Pendulum With Experimental Validation," *IEEE Access*, vol. 10, pp. 100857–100866, 2022, doi: 10.1109/ACCESS.2022.3208412.
17. S. I. Han and J. M. Lee, "Balancing and Velocity Control of a Unicycle Robot Based on the Dynamic Model," *IEEE Trans. Ind. Electron.*, vol. 62, no. 1, pp. 405–413, Jan. 2015, doi: 10.1109/TIE.2014.2327562.
18. A. Levant, "Sliding order and sliding accuracy in sliding mode control," *Int. J. Control*, vol. 58, no. 6, pp. 1247–1263, 1993, doi: 10.1080/00207179308923053.